

# Supporting Information

## **Threading Carbon Nanotubes through a Self-Assembled Nanotube**

Mingyang Ji,<sup>†</sup> McKensie L. Mason,<sup>†</sup> David A. Modarelli<sup>‡</sup> and Jon R. Parquette<sup>†\*</sup>

<sup>†</sup>Department of Chemistry, The Ohio State University, 100 W. 18th Ave. Columbus, Ohio 43210

<sup>‡</sup>Department of Chemistry and The Center for Laser and Optical Spectroscopy, Knight Chemical Laboratory, The University of Akron, Akron, Ohio 44325-3601

Email: parquette.1@osu.edu

## Table of Contents

Experimental Section	S4-S7
TEM images of pristine SWNTs	S8-S9
Zeta-potential intensity distributions	S10-S11
Raman spectra of SWNTs	S12
UV-vis and fluorescence emission spectra	S13
TEM image of SWNT/monomeric NDI-Bola composite	S14
UV-vis spectra of SWNT/NDI-Bola composites	S15
TEM image of SWNT/NDI-Bola in TFE	S16
XRD spectra	S17
CD spectra in water	S18
Zeta-potential titration curve of SWNT/NDI-Bola	S19
UV-vis spectra of NDI-Bola after ultracentrifuge	S20
DMT modulus AFM images	S21
Force-separation curves of DMT measurement	S22
UV-vis and fluorescence emission of SWNT/NDI-Bola/PPE-SO <sub>3</sub> Na	S23
TEM image of the mix of SWNTs and ultracentrifuged NDI-Bola	S24
TEM image of SWNT/NDI-Bola/PPE-SO <sub>3</sub> Na	S25
TEM image of de-bundled SWNTs	S26
TEM images of SWNT/NDI-Bola with dimensional measurements	S27
TEM images of NDI-Bola and SWNT/NDI-Bola without staining treatment	S28
Correlation between the G and 2D Raman modes	S29
TEM, fluorescence emission of NDI-Bola/PPE-SO <sub>3</sub> Na	S30
<sup>1</sup> H and <sup>13</sup> C NMR data	S31-S33



## EXPERIMENTAL SECTION

**Materials and Methods.** Atomic force microscopy (AFM) was conducted in tapping mode under a nitrogen atmosphere. All UV-vis spectra were recorded with a SHIMADZU UV-2450 spectrophotometer at 25 °C. All fluorescence spectroscopy was performed in a SHIMADZU RF-5301 spectrofluorophotometer using a cuvette with 3 mm pass length at 25 °C. Transmission electron microscopy (TEM) imaging was carried out with Technai G2 Spirit instrument operating at 80 kV. X-ray diffraction (XRD) measurements were taken on a Bruker D8 Advance Powder XRD in the flat plate reflection mode. <sup>1</sup>H and <sup>13</sup>C NMR were recorded at 400 MHz on a Bruker Avance III instrument. ESI mass spectra were recorded on a Bruker MicroTOF coupled with HPLC. Zeta-potential measurements were conducted on a Malvern Zetasizer NanoZS system with folded capillary zeta cells (DTS1070) at 25 °C. All reactions were performed under a nitrogen atmosphere. Dimethylformamide (DMF) was dried by distillation from MgSO<sub>4</sub>; dichloromethane was distilled from calcium hydride; chloroform was distilled from calcium carbonate. Chromatographic separations were performed on silica gel 60 (230-400 mesh, 60 Å) using indicated solvents.

**Preparation of SWNT/NDI-Bola Composites.** 10 mg of pristine SWNTs (AP-SWNT, Carbon Solutions, Inc.) were suspended in 40 mL of concentrated H<sub>2</sub>SO<sub>4</sub>/HNO<sub>3</sub> (3:1 v/v) and sonicated in a water bath for 3 h at 35-40 °C. The cut tubes were then further polished by stirring at 70 °C for 3 h.<sup>1</sup> The resulting suspension was then diluted with 200 mL of water and filtered by a 0.2-μm nylon membrane filter (Whatman). After washing with deionized water (100 mL), large SWNTs collected on membrane filter were further de-bundled in water (5 mL) via 1h sonication and dialyzed (Spectra/Por 3 dialysis membrane, molecular weight cut off: 3.5 kDa) against water (18.2 MΩ-cm, Millipore) for 2 d. The dialysate was centrifuged at 5000 rpm for 30 min to remove any precipitation and the resulting supernatant, with a SWNT concentration measured as 0.3 mg/mL, was collected for the following preparation.

NDI-Bola was synthesized according to our previous work.<sup>2</sup> Freeze-dried NDI-Bola (11.0 mg) was dissolved in 1.0 mL of HPLC-grade water to prepare homogeneous NDI-Bola (20 mM) solution. NDI-Bola dissolved in water completed the self-assembly within 12 h yielding well-defined nanotubes. Then, 1.0 mL of aqueous dispersion of polished SWNTs (0.3 mg/mL) was mixed with 1.0 mL of preformed NDI-Bola (11.0 mg/mL, 20 mM) nanotubes via three continuous, 10-min sonications at 10% of the maximum amplitude (Fisher Scientific 100 ultrasonic processor, 22.5 kHz) with 6-h intervals, yielding the SWNT/NDI-Bola composite as black viscous suspension. After incubation at 25 °C for 12 h, the SWNT/NDI-Bola composite formed self-supporting hydrogels, which were diluted with water (8 mL) and centrifuged at 5000 rpm for 10 min. After centrifuge, excess NDI-Bola (ca. 15 mol%) left in the resulting

supernatant was decanted, while the pellet of SWNT/NDI-Bola composite with a SWNT content estimated as 3 wt% was collected for the following study.

**Synthesis of conjugated polymer PPE-SO<sub>3</sub>Na.** The conjugated polymer PPE-SO<sub>3</sub>Na was synthesized via a modified method reported previously.<sup>3-4</sup> Under a nitrogen atmosphere, 8.8 g (80 mmol) of *p*-hydroquinone was rapidly dissolved in 100 mL of NaOH solution (10 wt%). Then, to the solution was added 160 mL of dioxane solution of 1,3-propane sultone (24.4 g, 200 mmol). The resulting mixture was stirred at 25 °C for 4 h and a precipitate formed. The acquired precipitate was vacuum filtered and washed with cold acetone to offer 1,4-di(propyloxysulfonate)benzene (**1**) as a white powder (yield: 85%). To 73 mL of a CH<sub>3</sub>COOH/H<sub>2</sub>SO<sub>4</sub>/H<sub>2</sub>O (40:3:30 v/v/v) mixture containing I<sub>2</sub> (3.86 g, 15.2 mmol) and KIO<sub>3</sub> (7.24 mmol) was added 5.77 g (14.5 mmol) of **1**. The resulting mixture was refluxed at 60°C for 12 h. After cooled in an ice-water bath, the reaction mixture was filtered and then washed with cold ethanol to give 1,4-diiodo-2,5-di(propyloxysulfonate)benzene (**2**) as fine white powder with high purity (yield: 70%).

1,4-Diethynylbenzene (0.1 g, 0.75 mmol) and **2** (0.5 g, 0.78 mmol) were dissolved in 20 mL of H<sub>2</sub>O/DMF (1:1 v/v) under an argon atmosphere. The resulting clear solution was deoxygenated by three cycles of vacuum-argon cycling. Then, to the deoxygenated solution was added 10 mL of diisopropylamine/DMF (1:1 v/v) containing Pd(PPh<sub>3</sub>)<sub>4</sub> (30.0 mg, 26.0 μM) and CuI (10.0 mg, 45.0 μM) under stirring. The resulting mixture was deoxygenated again by vacuum-argon cycling for three times and was then heated to 55 °C for 20 h under a positive pressure of argon. After reaction, the cooled solution was slowly added to 500 mL of a methanol/acetone/ether mixture (10:40:50 v/v/v) and a yellow precipitate formed. The resulting precipitate was filtered out and redissolved in 100 mL of H<sub>2</sub>O/methanol (70:30 v/v), and was then treated with 0.1 g of Na<sub>2</sub>S. Then, the concentrated solution was filtered through quantitative filter papers and glass fiber filters (2.7 μm, Whatman). The filtered solution was precipitated in a large volume of methanol/acetone/ether (10:40:50 v/v/v), then the resulting precipitate was dissolved in water and dialyzed against water (18.2 MΩ·cm, Millipore) for three days. The dialysate was freeze-dried to give the product as yellow solid. <sup>1</sup>H NMR (400 MHz, DMSO-*d*<sub>6</sub>) 2.07 (t, 4H), 2.69 (t, 4H), 4.16 (t, 4H), 7.19 (s, 2H), 7.59 (4H). The molecular weight of PPE-SO<sub>3</sub>Na was determined by MALDI-TOF: M<sub>w</sub> = 5.76 × 10<sup>4</sup>, PDI = 1.11, sinapinic acid as the matrix.

**Preparation of the SWNT/NDI-Bola/PPE-SO<sub>3</sub>Na Composite.** Under vortexing, different amount of PPE-SO<sub>3</sub>Na (10 mM based on the repeat unit) was added to re-suspended SWNT/NDI-Bola in monomeric molar ratio of 10:0.5, 10:1, and 10:2 (NDI-Bola/PPE-SO<sub>3</sub>Na). For the ternary SWNT/NDI-Bola/PPE-SO<sub>3</sub>Na composite, 10:0.5, 10:1, and 10:2 indicate the feeding ratio of NDI-Bola in SWNT/NDI-Bola to PPE-SO<sub>3</sub>Na monomer for simplicity. Considering the loss of NDI-Bola after centrifuge, the actual molar ratios in corresponding SWNT/NDI-Bola/PPE-SO<sub>3</sub>Na were ca. 10:0.6, 10:1.2 and 10:2.4 (NDI-

Bola/PPE-SO<sub>3</sub>Na). After incubating at 20 °C for 12 h, the SWNT/NDI-Bola/PPE-SO<sub>3</sub>Na composite was diluted with water (2 mL) and centrifuged at 5000 rpm for 15 min. The resultant supernatants were decanted, and pellets of SWNT/NDI-Bola/PPE-SO<sub>3</sub>Na composite were collected for the following study.

**Zeta-Potential Measurements.** Zeta-potential measurements were conducted on a Malvern Zetasizer NanoZS system with irradiation from a 632.8 nm He-Ne laser. Freshly diluted samples were filled in folded capillary zeta cells (DTS1070) and measured in the mixed mode combining fast and slow field reversal to eliminate electroosmotic effects.

**Fluorescence Spectroscopy Measurements.** Aqueous samples for steady state fluorescence study (the concentration of NDI-Bola in all samples was 1 mM) were prepared by dilution from 20 mM of NDI-Bola or pellets of SWNT/NDI-Bola and SWNT/NDI-Bola/PPE-SO<sub>3</sub>Na composites after centrifuge (5000 rpm). All samples were equilibrated for 24 h before measurements. All fluorescence emission spectra were measured with excitation at 350 nm.

**Atomic Force Microscopy (AFM) Imaging and PeakForce Quantitative Nanomechanical Mapping (QNM) Measurements.** AFM images were collected on a Bruker AXS Dimension Icon Atomic Force Microscope under a nitrogen atmosphere in tapping mode using silicon tips (SCANASYST-AIR or RTESPA-300, Bruker). The SWNT/NDI-Bola composite was collected in pellets after centrifuge and diluted (the concentration of NDI-Bola in all samples was 2 mM) to cast on freshly cleaved mica for imaging. The scanning speed was at a line frequency of 0.2 Hz, and the original images were sampled at a resolution of 512 × 512 pixels. All PeakForce QNM measurements were carried out by using RTESPA-300 probes (Bruker) with a nominal cantilever spring constant ( $k$ ) as 40 N/m, which is suitable for sample modulus between 200 MPa to 2 GPa. In order to obtain quantitative results from PeakForce QNM, each probe was calibrated through the absolute method respectively. Firstly, an indentation was taken on a hard sapphire sample (Bruker SAPPHIRE-15M) to calibrate the deflection sensitivity of the probes found to be 60-90 nm/V. Then, cantilever spring constants were measured by thermal tuning and found to be 35-60 N/m depending on the actual mechanical properties of each probe. Finally, the tip end radius was measured by scanning a titanium roughness sample as the tip calibration artifact (Bruker RS-15M).

In PeakForce QNM mode, the piezo-scanner oscillates at a frequency (2 kHz) far below the resonance frequency of cantilever  $f_0$ , at which the traditional tapping mode AFM operates. During the line-by-line scanning, continuous nanoindentations of the sample enable the capture of force-separation curves in a point-by-point fashion.<sup>5-6</sup> Young's modulus is then calculated from the unloading portion of these force-separation curves using the Derjaguin-Muller-Toporov (DMT) model. According to this approach, the reduced Young's modulus ( $E_r$ ) is given by equation (1):

$$E_r = \frac{3(F_{tip} - F_{adh})}{4\sqrt{Rd^3}} \quad (1)$$

where  $F_{tip}$  is the force on the AFM tip,  $F_{adh}$  is the adhesive force between the AFM tip and sample,  $R$  is the AFM tip radius, and  $d$  is the penetration depth. The reduced Young's modulus is related to the sample Young's modulus ( $E_s$ ) through equation (2):

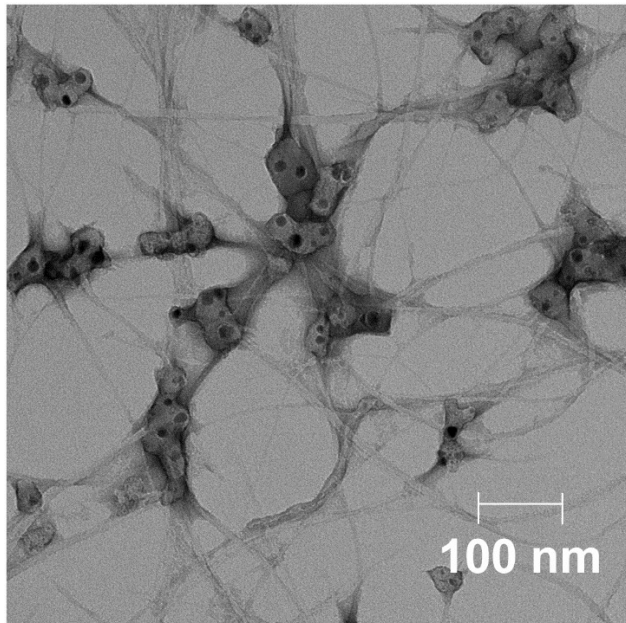
$$\frac{1}{E_r} = \frac{(1 - \nu_s^2)}{E_s} + \frac{(1 - \nu_i^2)}{E_i} \quad (2)$$

where  $E_i$  is the indenter Young's modulus,  $\nu_i$  is the Poisson's ratio of the indenter and  $\nu_s$  is the Poisson's ratio of the sample. Provided that  $E_i \gg E_s$ , the second term on the right-hand side of equation (2) is negligible, then the Young's modulus of the test specimen is determined by equation (3):

$$E_r = \frac{E_s}{1 - \nu_s^2} \quad (3)$$

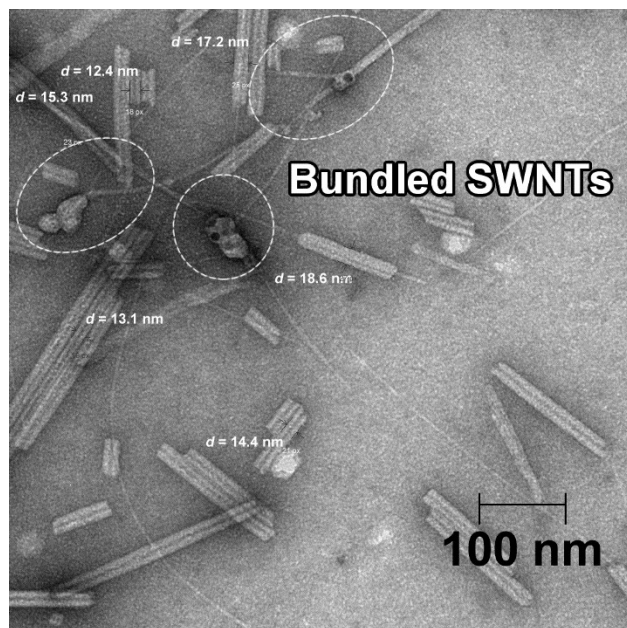
**Raman Spectroscopy Measurements.** The Raman spectra were collected at excitation laser wavelengths of 785.0 nm ( $E_{laser} = 1.58$  eV) and 514 nm ( $E_{laser} = 2.41$  eV) on a Renishaw Raman IR microprobe equipped with a CCD detector. All Raman spectra were collected at room temperature and using a backscattering geometry. Different acquisition times between 2-10 s were used for each sample to optimize the signal-to-noise ratio of the Raman spectra. The  $50 \times$  long-working-distance objective was dedicated to liquid samples in a 10-mm quartz cuvette. The position of all Raman peaks was verified by calibrating the spectral positions in respect to internal silicon reference peak at  $521 \text{ cm}^{-1}$ .

**X-ray Diffraction (XRD) Measurement.** Preassembled NDI-Bola nanotubes (20 mM) and SWNT/NDI-Bola collected from pellets after centrifuge (5000 rpm) were dropped and completely dried on the cleaned surface of monocrystalline silicon wafer, which was fixed on the XRD sample holder. XRD patterns were recorded on a Bruker D8 powder diffractometer operating at 40 kV and 25 mA, using  $\text{CuK}\alpha$  radiation ( $\lambda = 1.5418 \text{ \AA}$ ). Data were collected from  $2^\circ$  to  $55^\circ$  with a sampling interval of  $0.02^\circ$  per step and a counting rate of 2 s per step.

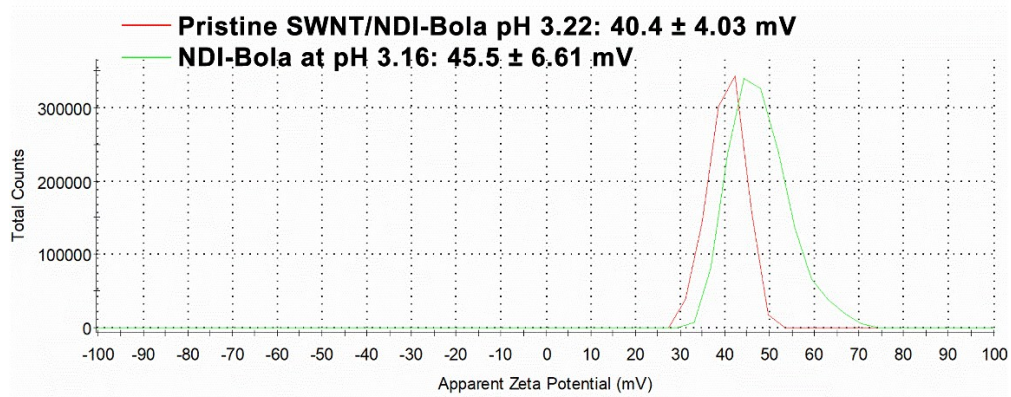


**Figure S1.** TEM image of pristine SWNTs dispersed by SDS. Pristine SWNTs (10 mg) were dispersed in 10 mL of SDS solution (1 wt%) by sonication for 3 h. The obtained dispersion was centrifuged at 5000 rpm for 1 h to collect the supernatant for TEM imaging.

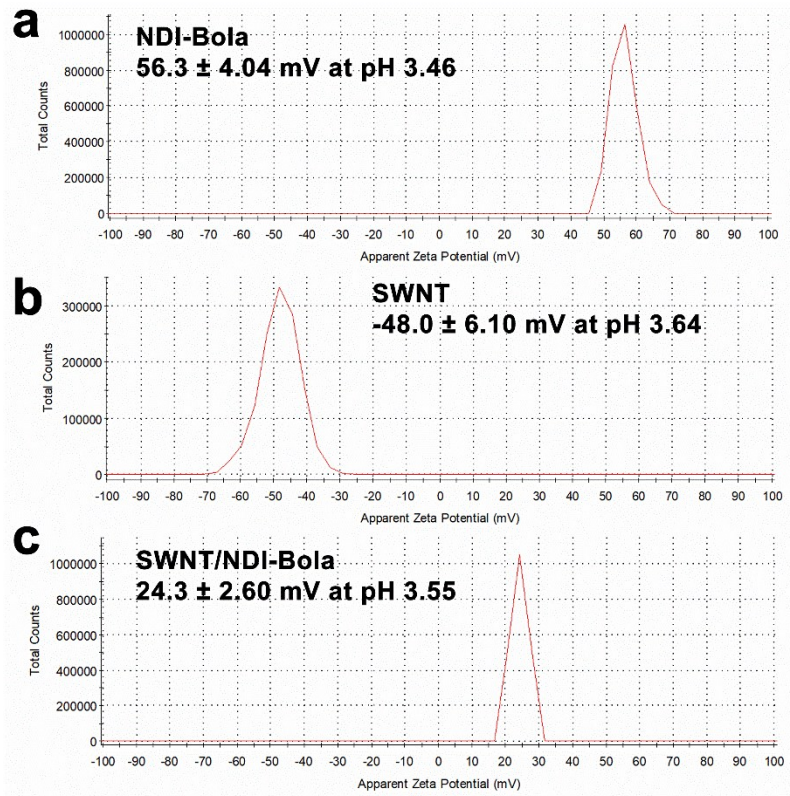




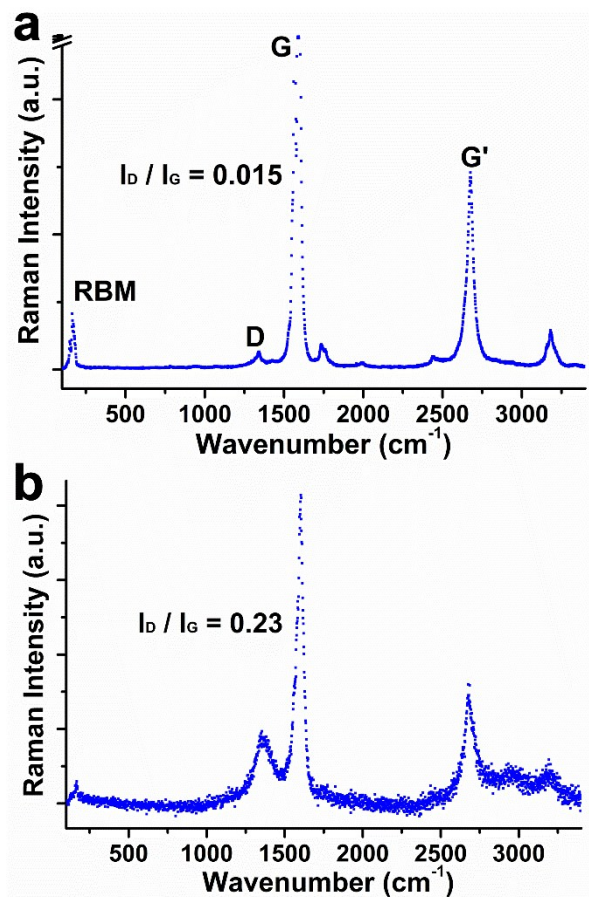
**Figure S2.** TEM image of pristine SWNTs dispersed in preformed NDI-Bola nanotubes. Pristine SWNTs (0.3 mg) were dispersed in 1 mL of preformed NDI-Bola nanotubes (10 mM) by 8 consecutive sonications with 6 h intervals. The obtained homogeneous dispersion was diluted by 9 mL of H<sub>2</sub>O and centrifuged at 5000 rpm for 1 h to collect the supernatant for TEM imaging.



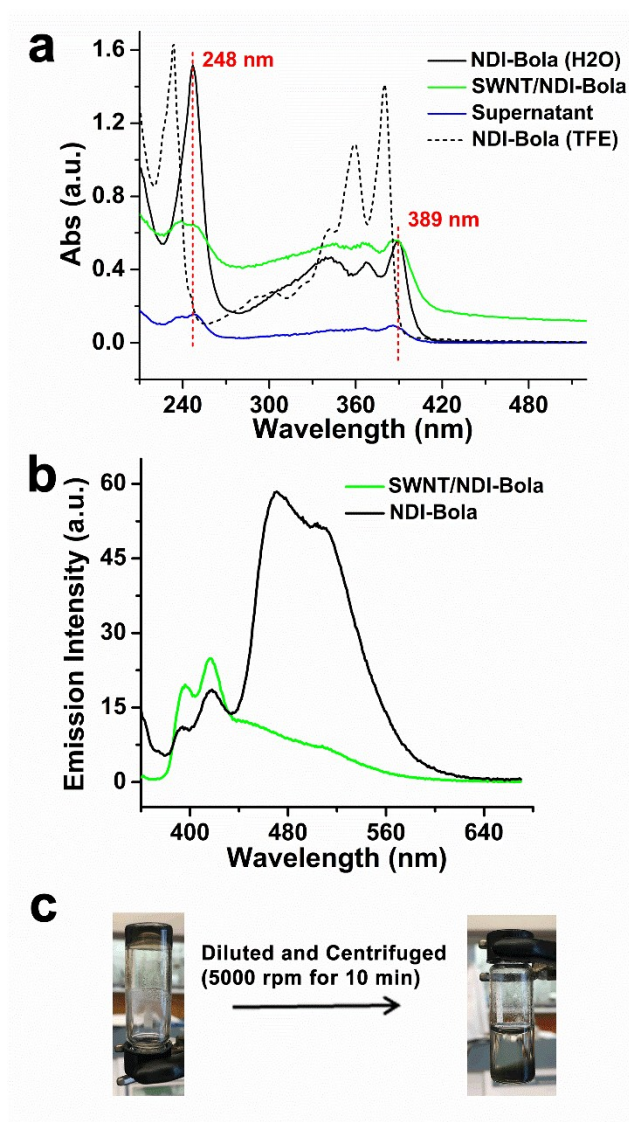
**Figure S3.** Zeta potential distributions of NDI-Bola nanotubes (1 mM) at pH 3.16 and pristine SWNTs dispersed by preformed NDI-Bola nanotubes (pristine SWNT/NDI-Bola). After sonication, the resulting dispersion of pristine SWNT/NDI-Bola was diluted to 1 mM (with respect NDI-Bola) with a natural pH 3.22 for zeta-potential measurements.



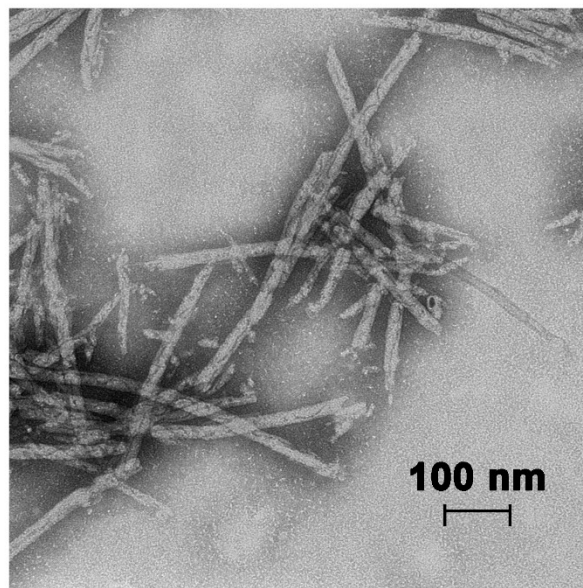
**Figure S4.** Zeta potential intensity distributions of (a) NDI-Bola (2 mM, pH 3.46), (b) debundled SWNT (0.3 mg/mL, pH 3.64) and (c) SWNT/NDI-Bola (2 mM with respect to NDI-Bola, pH 3.55) in water.



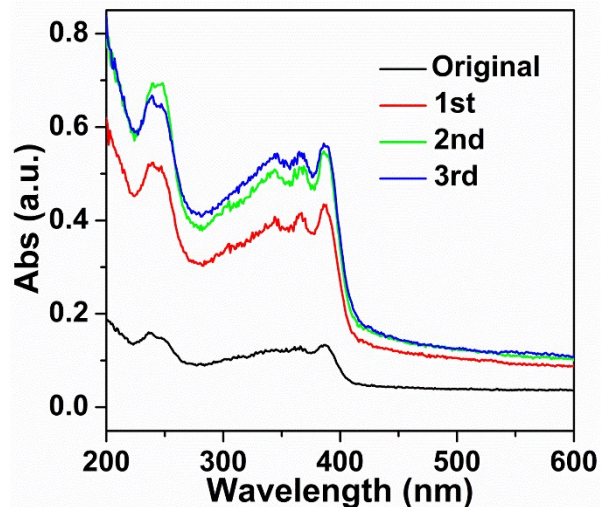
**Figure S5.** Raman spectra (excited with a 514 nm laser) of (a) pristine SWNTs powder and (b) de-bundled SWNTs powder after acid treatment ( $\text{H}_2\text{SO}_4/\text{HNO}_3$  3:1). The diameter of SWNTs was estimated as 1.6 nm, based on the RBM peak at  $167.8 \text{ cm}^{-1}$  in (a).<sup>7</sup> The D/G ratio increased from 0.015 for pristine SWNTs in (a) to 0.23 for de-bundled SWNTs in (b), which demonstrates the intensified structural defect on SWNTs after acid treatment.



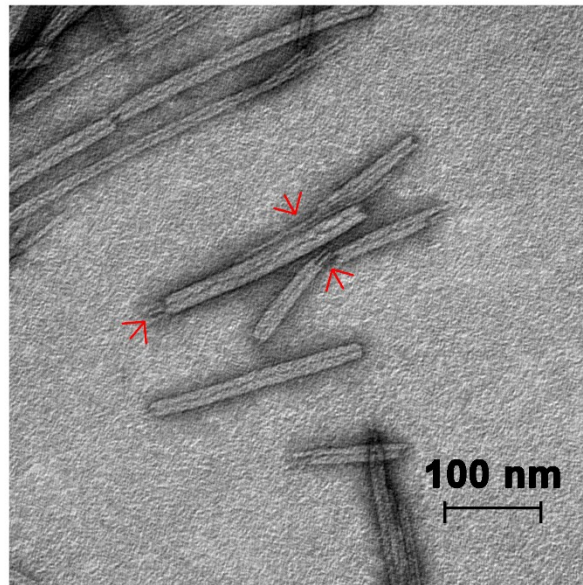
**Figure S6.** (a) UV-vis spectra of pre-assembled NDI-Bola nanotubes in water (solid black), monomolecular NDI-Bola in TFE (dashed black), the aqueous dispersion of SWNT/NDI-Bola composite (green) collected from pellets after centrifuge at 5000 rpm and the corresponding supernatant (blue). Except for the supernatant, the concentration of NDI-Bola in all samples was 250  $\mu$ M. (b) Fluorescence emission spectra of NDI-Bola nanotubes in water (black) and aqueous dispersion of SWNT/NDI-Bola composite (green). The concentration of NDI-Bola in all samples was 1 mM. All samples were excited at 350 nm. (c) After incubating at 25  $^{\circ}$ C for 12 h, the mixture of SWNTs and NDI-Bola nanotubes formed self-supporting hydrogels. The resulting hydrogel was diluted with water and centrifuged at 5000 rpm for 10 min to collect the SWNT/NDI-Bola composite in the pellets.



**Figure S7.** Freeze-dried NDI-Bola (5.5 mg) was dissolved in 0.5 mL of aqueous dispersion of SWNTs (0.3 mg/mL) and the mixture was sonicated until all the solid dissolved. After incubating at 25 °C for 48 h, resultant mixture was diluted to 1 mM with respect to NDI-Bola and applied to a carbon-coated copper grid for TEM imaging. 2% (w/w) uranyl acetate as the negative stain. Using monomeric NDI-Bola instead of preformed nanotubes generated randomly aggregated nanorods, probably resulting from the overwhelming hydrophobic interaction between SWNTs and NDI chromophores against the self-assembly of NDI-Bola.

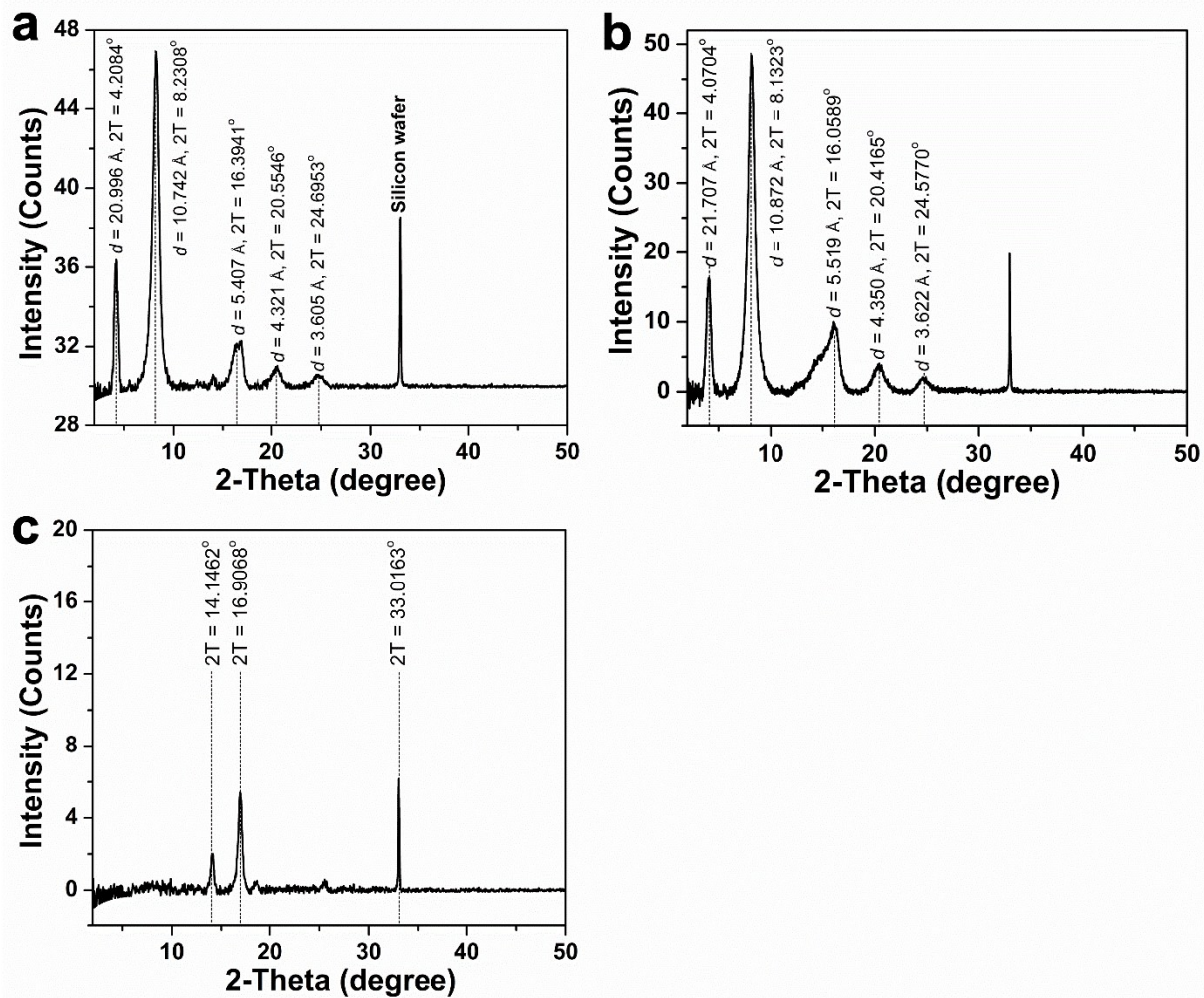


**Figure S8.** UV-vis spectra of aqueous dispersions of SWNT/NDI-Bola composite along with repeated sonications and incubations. Firstly, 0.1 mL of preformed NDI-Bola (20 mM) nanotubes was mixed with 0.1 mL of aqueous dispersion of SWNTs (0.3 mg/mL) via 10-min sonication (10% amplitude). Then, the resultant mixture was diluted with water (7.8 mL) and centrifuged at 5000 rpm for 10 min. The resultant supernatant was decanted, and the pellet was redispersed in water (8 mL) to collect the original (black) spectrum of SWNT/NDI-Bola composite. Following the same preparation, the spectra of SWNT/NDI-Bola composites were taken after 6-h incubation (1st, red), second 10-min sonication and subsequent 6-h incubation (2nd, green), and third 10-min sonication and subsequent 12-h incubation (3rd, blue), respectively.

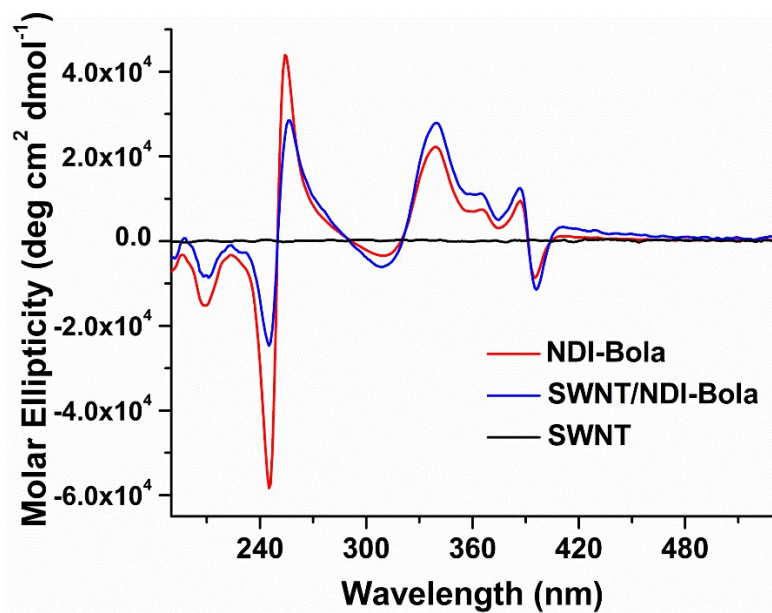


**Figure S9.** The SWNT/NDI-Bola composite collected in the pellet after centrifugation (5000 rpm for 10 min) was transferred into TFE. After incubating at 25 °C for 30 min, the TFE dispersion of SWNT/NDI-Bola was applied to a carbon-coated copper grid for TEM imaging. Red arrows indicate the part of SWNTs re-exposed to the environment due to the partly dissociation of NDI-Bola in TFE.

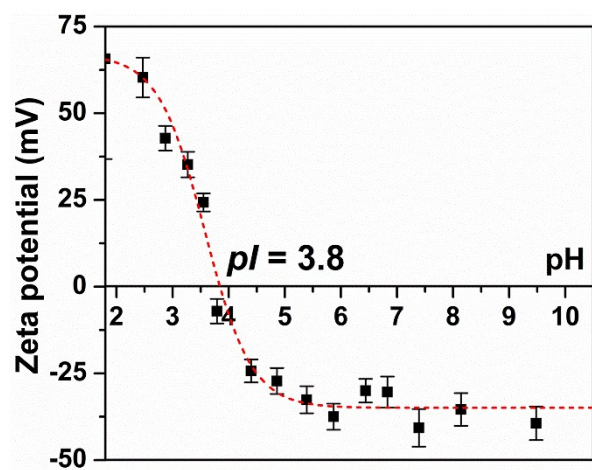




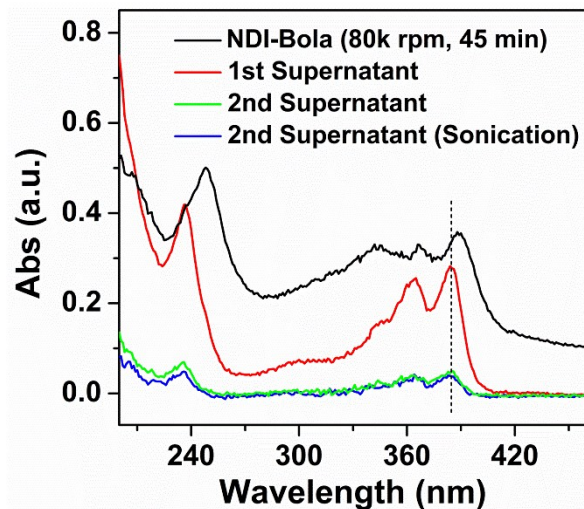
**Figure S10.** XRD patterns of (a) SWNT/NDI-Bola and (b) NDI-Bola nanotubes dried on monocrystalline silicon wafer and (c) silicon wafer as the substrate.



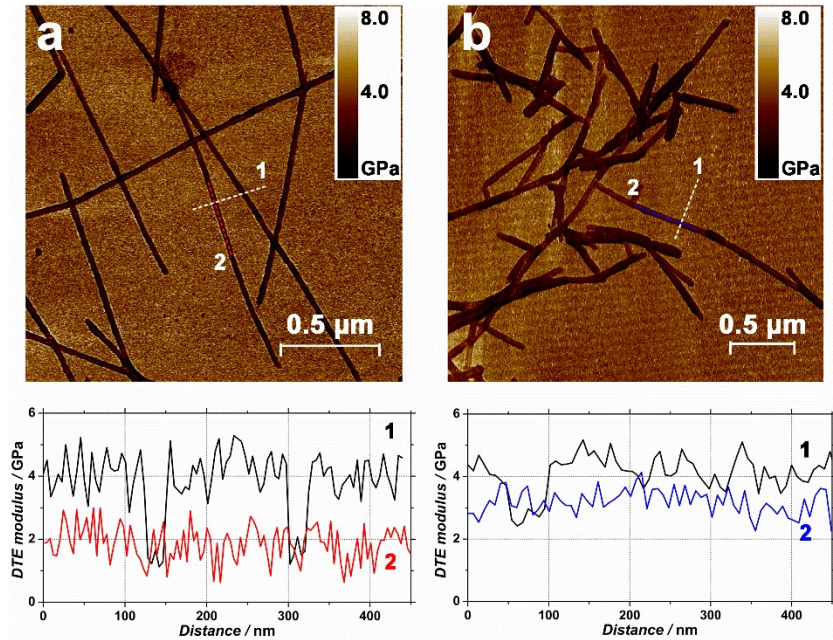
**Figure S11.** CD spectra of NDI-Bola nanotubes (red, 1 mM), the SWNT/NDI-Bola composite (blue, 1 mM with respect to NDI-Bola), and SWNTs (0.3 mg/mL) in water.



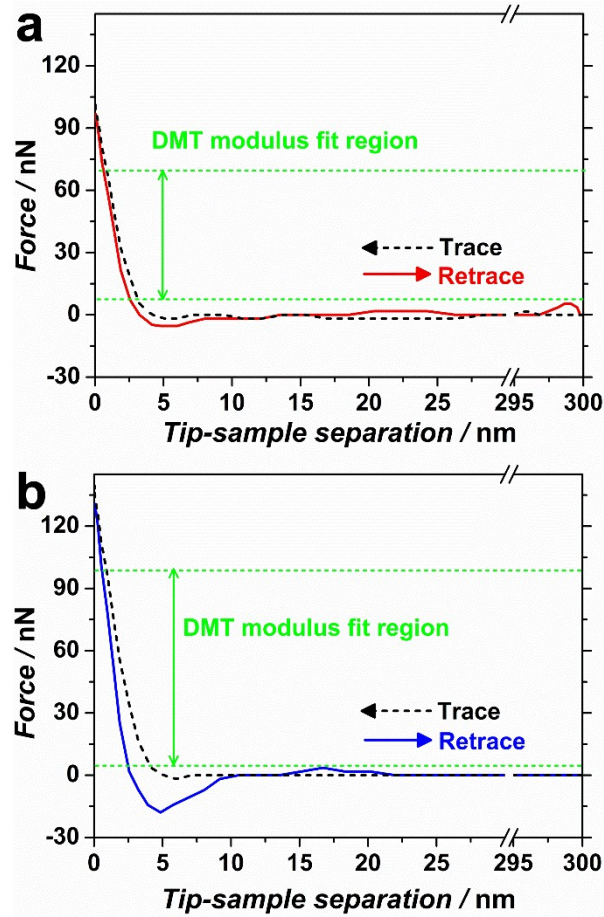
**Figure S12.** Zeta potential titration curve of SWNT/NDI-Bola (2 mM respect to NDI-Bola) composite in water at 25 °C. The titration was performed using 1 M HCl and 1 M NaOH. The dashed curve is given for eye guidance.



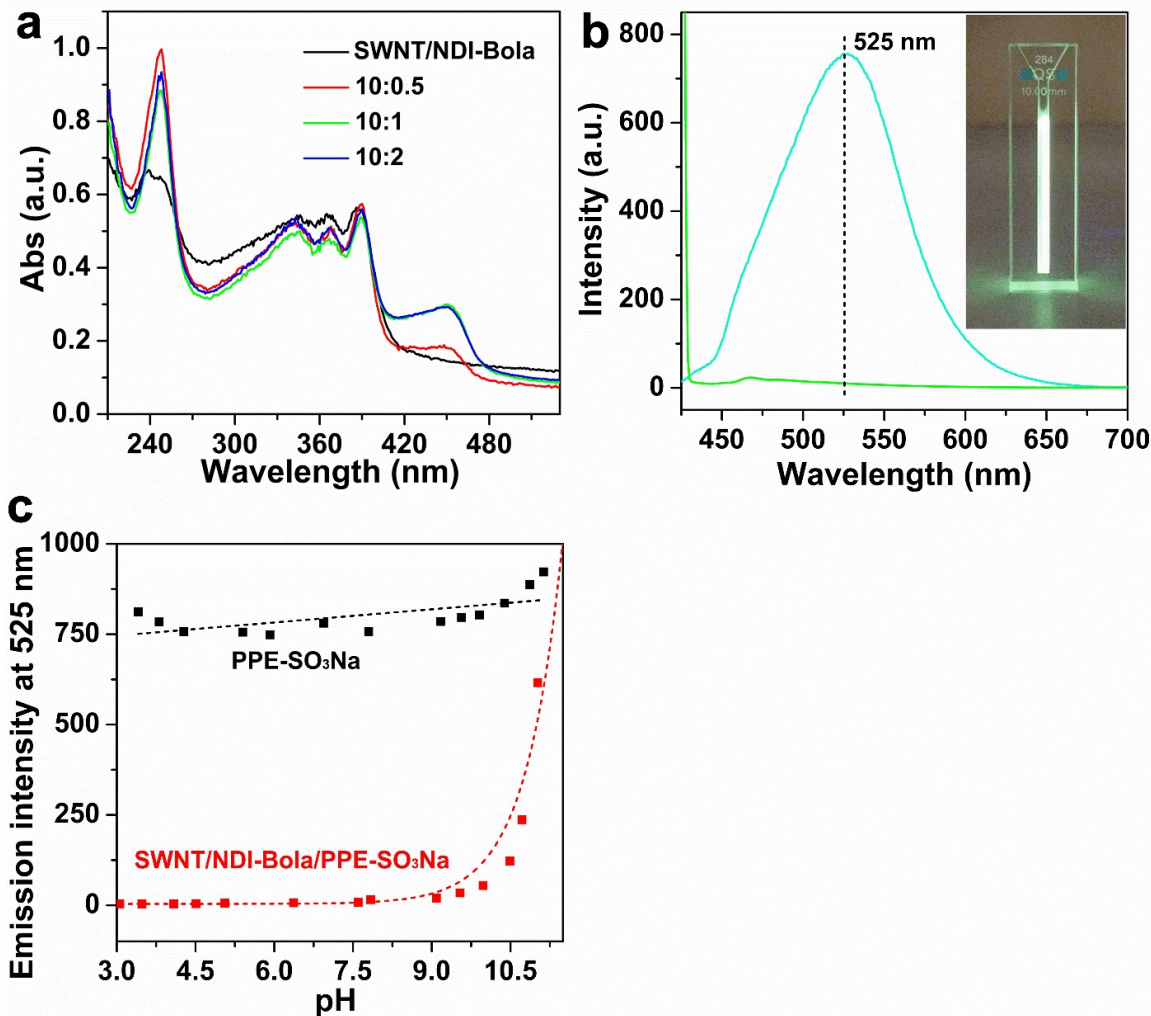
**Figure S13.** UV-vis spectra of NDI-Bola pellets (black) after ultracentrifuge (80k rpm for 45 min) and the corresponding supernatant (red) which revealed the existence of extra NDI-Bola monomers. After the first ultracentrifuge, the corresponding supernatant displayed characteristic peaks attributed to monomolecular form of NDI-Bola. The pellet of NDI-Bola nanotubes was redispersed in water (ca. 20 mM) and incubated at 25 °C for 24 h, then, a portion of the aqueous dispersion of NDI-Bola nanotubes was sonicated at 10% maximum amplitude for 15 min. After sonication, the resultant dispersion and the original dispersion without sonication were taken to second ultracentrifuge (80k rpm, 45 min). After the second ultracentrifuge, the absorption spectra of corresponding supernatants from samples with (blue) and without (green) sonication were measured, respectively.



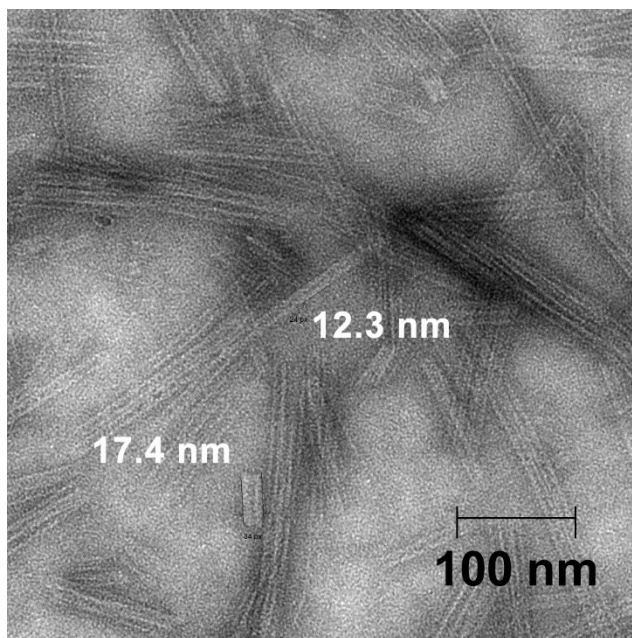
**Figure S14.** DMT modulus AFM images of (a) NDI-Bola nanotubes and (b) SWNT/NDI-Bola composite. Insets: DMT modulus profiles along NDI-Bola (red) and SWNT/NDI-Bola (blue), and the cross-sections drawn over the nanotubes in (a) and (b) (black). Modulus profiles revealed variations on measurements based on the DMT model, which assumes the predominant contact is between a spherical tip of defined radius and a flat surface, probably resulting from incomplete contact between the probe tip and the surface of nanotubes during scanning. When the tip comes to contact with side walls of nanotubes along with its line-by-line movements during scanning, the contact area in this incipient situation is deviated from the presumption of the DMT model which renders the measurements at the edge of nanotubes less convincing. In contrast, the minimum modulus values in the profiles drawn over nanotubes (black profiles in insets), corresponding to measurements right above the center of nanotubes, should be less affected by the geometric artefacts observed on the side walls of nanotubes and were taken as dependable nanotube modulus.<sup>8</sup>



**Figure S15.** Force-separation curves of (a) NDI-Bola and (b) SWNT/NDI-Bola while approaching the surface (trace) and withdrawal (retrace). Retrace curves within dashed green regions correspond to the fitting of experimental results to the DMT model. Automatic analyses on the force-separation curves by the software (NanoScope Analysis 1.40, Bruker) enable the extraction of the height, elastic modulus, adhesion force, deformation and dissipation simultaneously through the DMT model. The Young's modulus is obtained by fitting the retrace curves with a Poisson's ratio of 0.3.

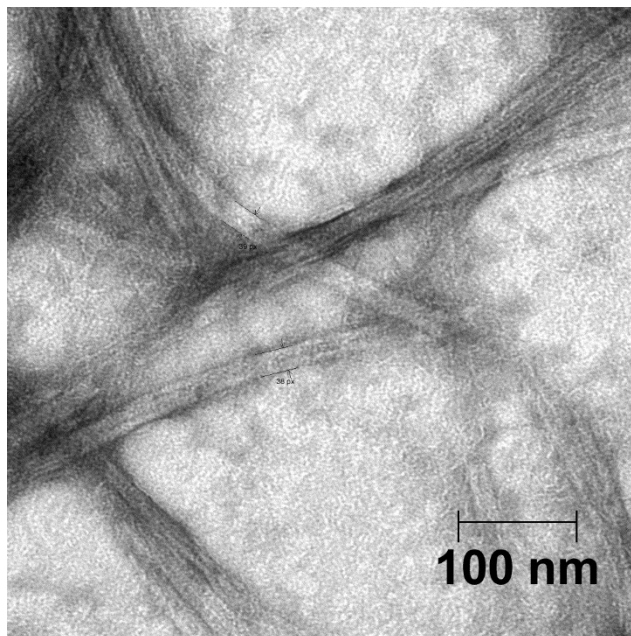


**Figure S16.** (a) UV-vis spectra of SWNT/NDI-Bola (black) and SWNT/NDI-Bola/PPE-SO<sub>3</sub>Na in molar ratios (NDI-Bola in composite/PPE-SO<sub>3</sub>Na) of 10:0.5 (red), 10:1 (green) and 10:2 (blue) in water. The varied ratios of SWNT/NDI-Bola/PPE-SO<sub>3</sub>Na indicate the feeding ratio of NDI-Bola in composite to PPE-SO<sub>3</sub>Na monomer. Considering the loss of NDI-Bola in the supernatant during preparation of SWNT/NDI-Bola, the final molar ratios in corresponding SWNT/NDI-Bola/PPE-SO<sub>3</sub>Na were 10:0.6, 10:1.2 and 10:2.4. (b) Steady state fluorescence spectra of SWNT/NDI-Bola/PPE-SO<sub>3</sub>Na (10:1, pH 6.4, green) and PPE-SO<sub>3</sub>Na (100 μM with maximum emission at 525 nm, pH 6.2, cyan) excited at 420 nm in water. (c) The dependence of fluorescence emission of SWNT/NDI-Bola/PPE-SO<sub>3</sub>Na (10:1, red) and PPE-SO<sub>3</sub>Na (100 μM, black) at 525 nm on pH. The concentration of NDI-Bola and PPE-SO<sub>3</sub>Na in SWNT/NDI-Bola/PPE-SO<sub>3</sub>Na (10:1) were 1 mM and 100 μM, respectively. Inset: Photograph of PPE-SO<sub>3</sub>Na (100 μM in water) under illumination of UV lamp at 365 nm.

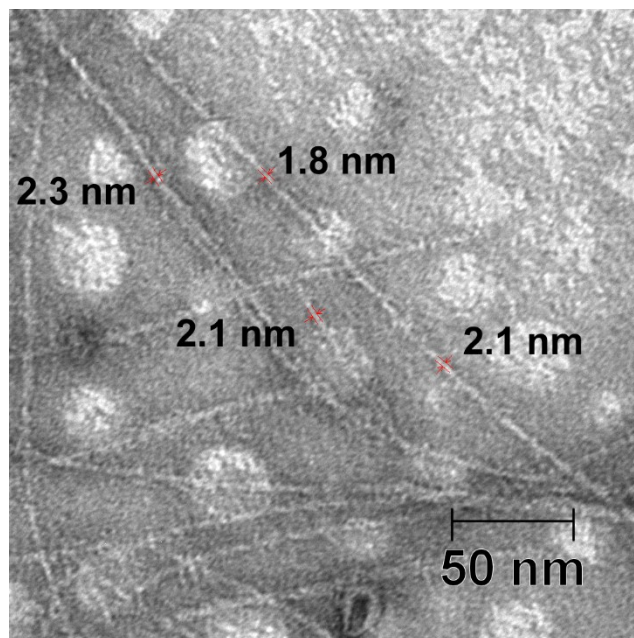


**Figure S17.** After removing free NDI-Bola monomer via ultracentrifuge (80k rpm, 45 min), redispersed NDI-Bola nanotubes were mixed with polished SWNTs through as described sonication-assisted incubation. After incubation, the resulting mixture was also diluted with water (1 mM) and centrifuged at 5000 rpm, expecting to collect the SWNT/NDI-Bola in the pellet. However, the pelleting was unsuccessful as hardly any composite was able to be collected. The TEM image of this mixture revealed that most of NDI-Bola nanotubes, except rare short segments with a similar diameter of SWNT/NDI-Bola indicating a bilayer coating, remained their monolayer structure with a diameter of ca. 12 nm.

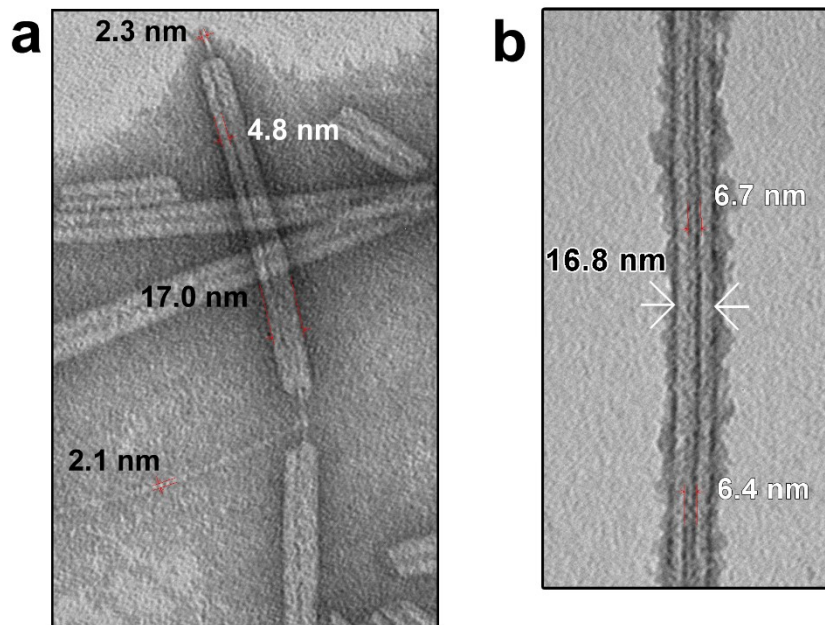




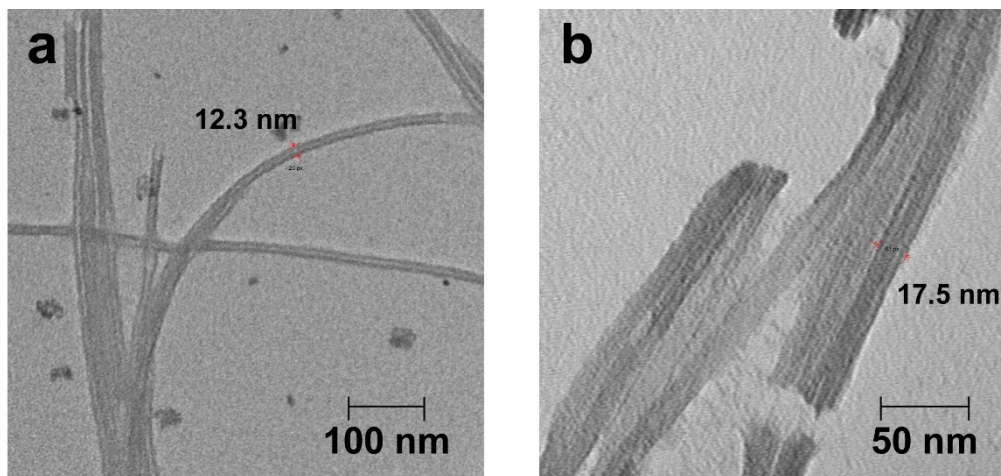
**Figure S18.** TEM image of SWNT/NDI-Bola/PPE-SO<sub>3</sub>Na (10:1 NDI-Bola/PPE-SO<sub>3</sub>Na). Under vortexing, PPE-SO<sub>3</sub>Na was added to SWNT/NDI-Bola in a molar ratio of 10:1 (NDI-Bola/PPE-SO<sub>3</sub>Na). After incubation and centrifuge, the SWNT/NDI-Bola/PPE-SO<sub>3</sub>Na was diluted with water (1 mM) for TEM imaging. 2% (w/w) uranyl acetate as the negative stain.



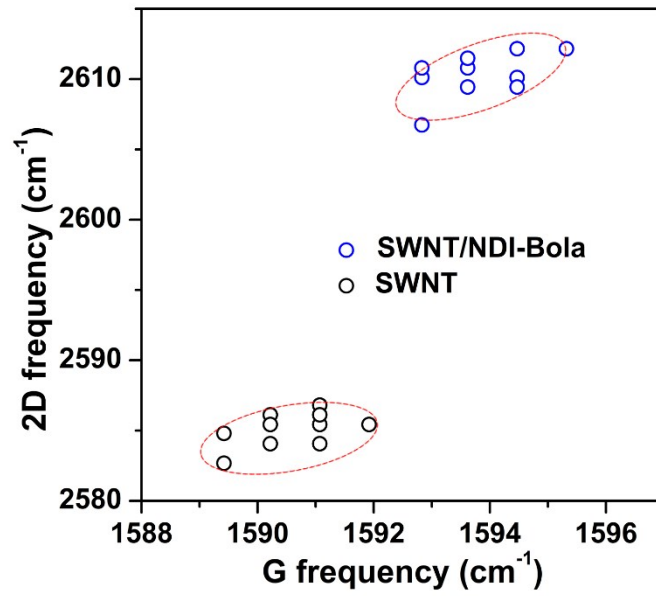
**Figure S19.** TEM image of de-bundled SWNTs after acid treatment, dimensional measurements indicate a diameter ca. 2 nm. 2% (w/w) uranyl acetate as the negative stain.



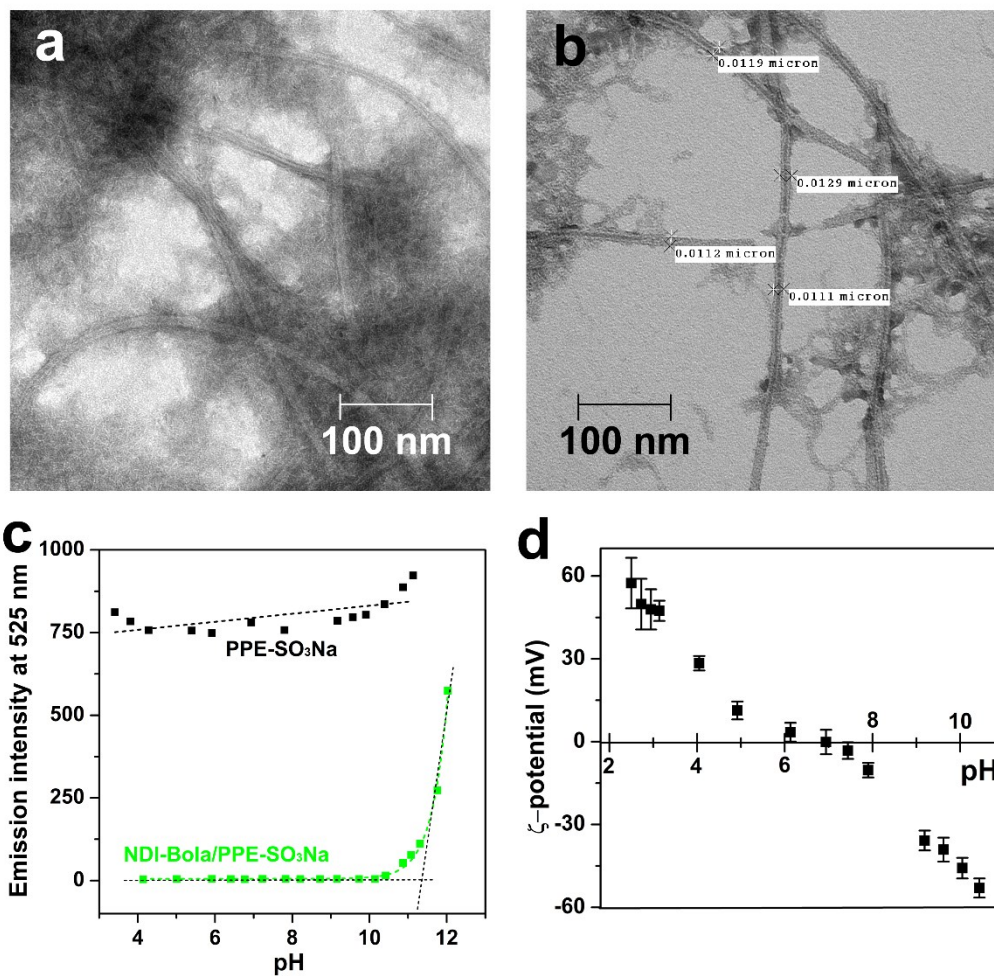
**Figure S20.** TEM images of SWNT/NDI-Bola with dimensional measurements, 2% (w/w) uranyl acetate as the negative stain. As shown in (a), rather than locating at the exact center of the inner channel, SWNT locates much closer to one of the NDI-Bola walls in this cross-sectional observation, leaving the other wall measured as 4.8 nm. As a comparison, the SWNT/NDI-Bola in (b) shows a rare situation which both walls by NDI-Bola can be clearly distinguished from SWNT, allowing a direct measurement on the inner channel as 6-7 nm.



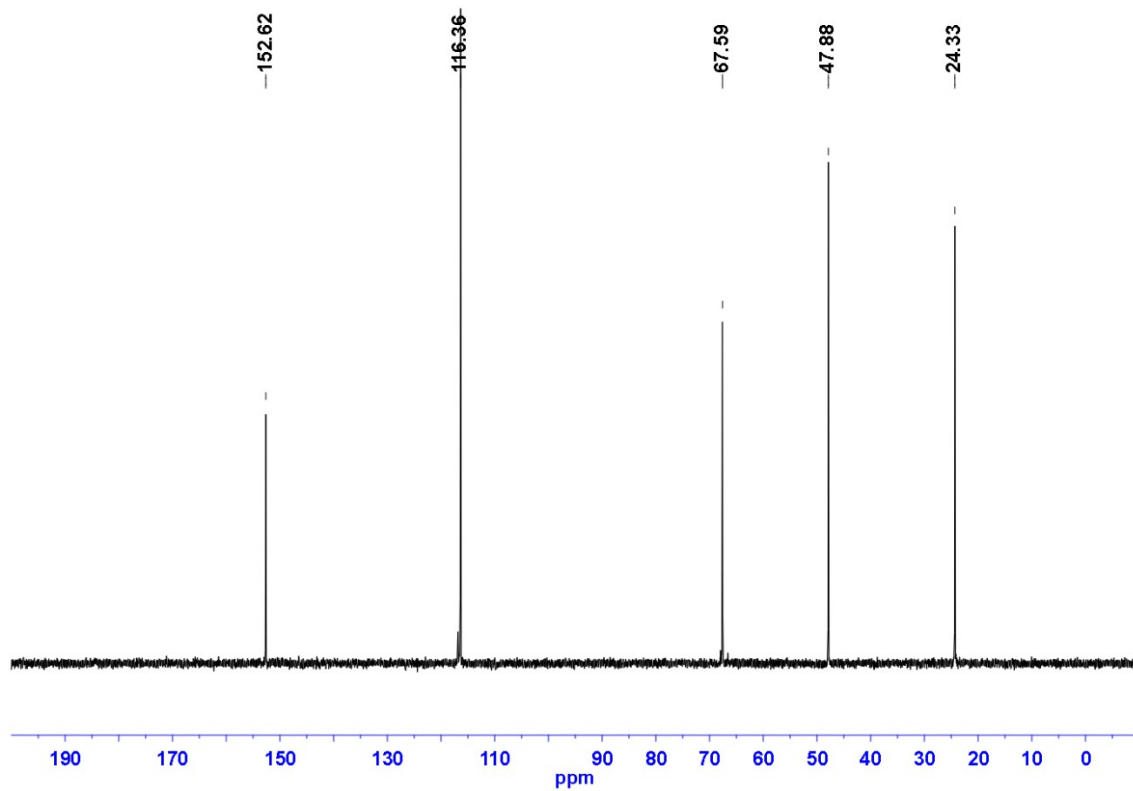
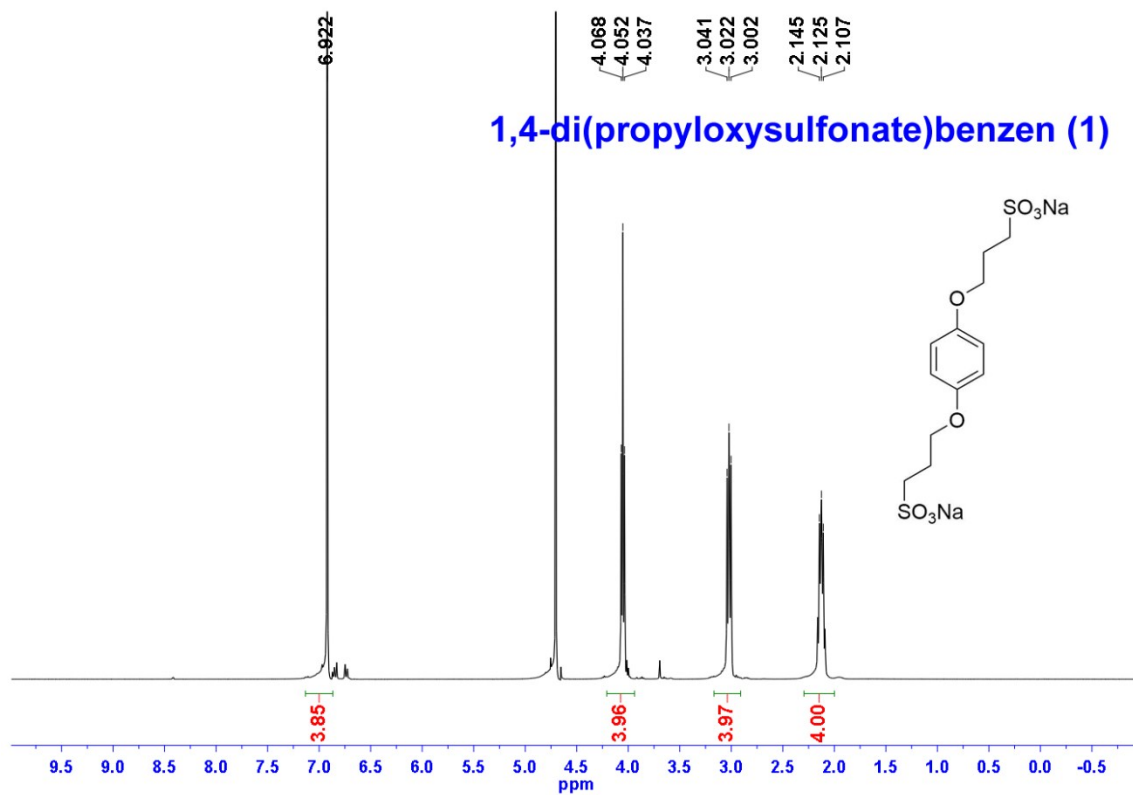
**Figure S21.** TEM images of (a) NDI-Bola and (b) SWNT/NDI-Bola without staining treatment. Both images were taken under the accelerating voltage of the microscope as 80 kV. Although suffered from less discernible boundaries, the morphology and dimensions here generally agree with the measurements on stained samples.

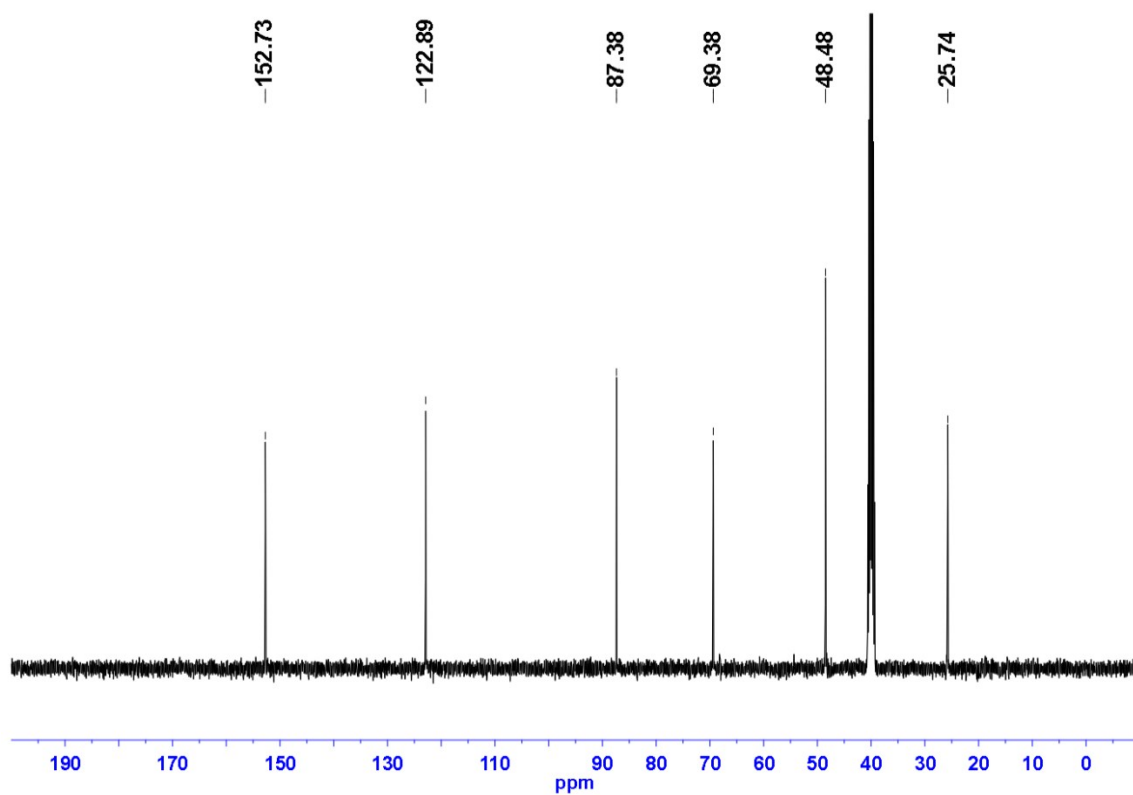
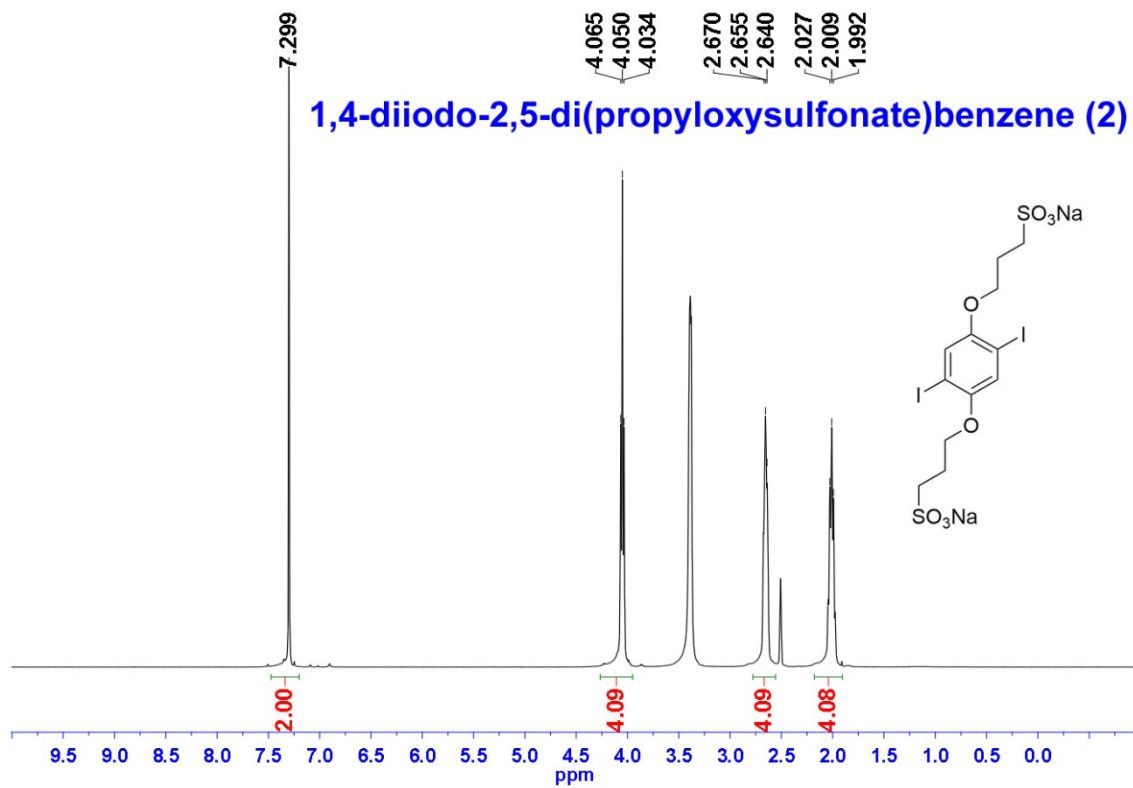


**Figure S22.** Correlation between the G and 2D Raman modes of SWNT (black) and SWNT/NDI-Bola (blue).

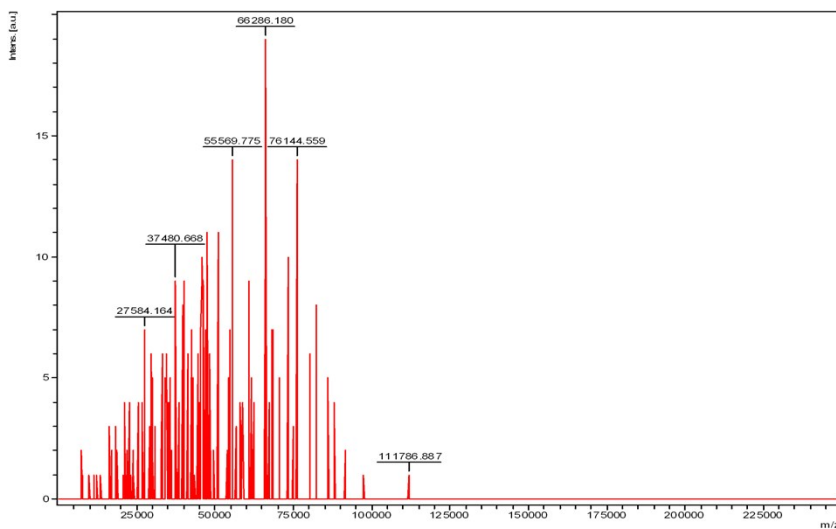
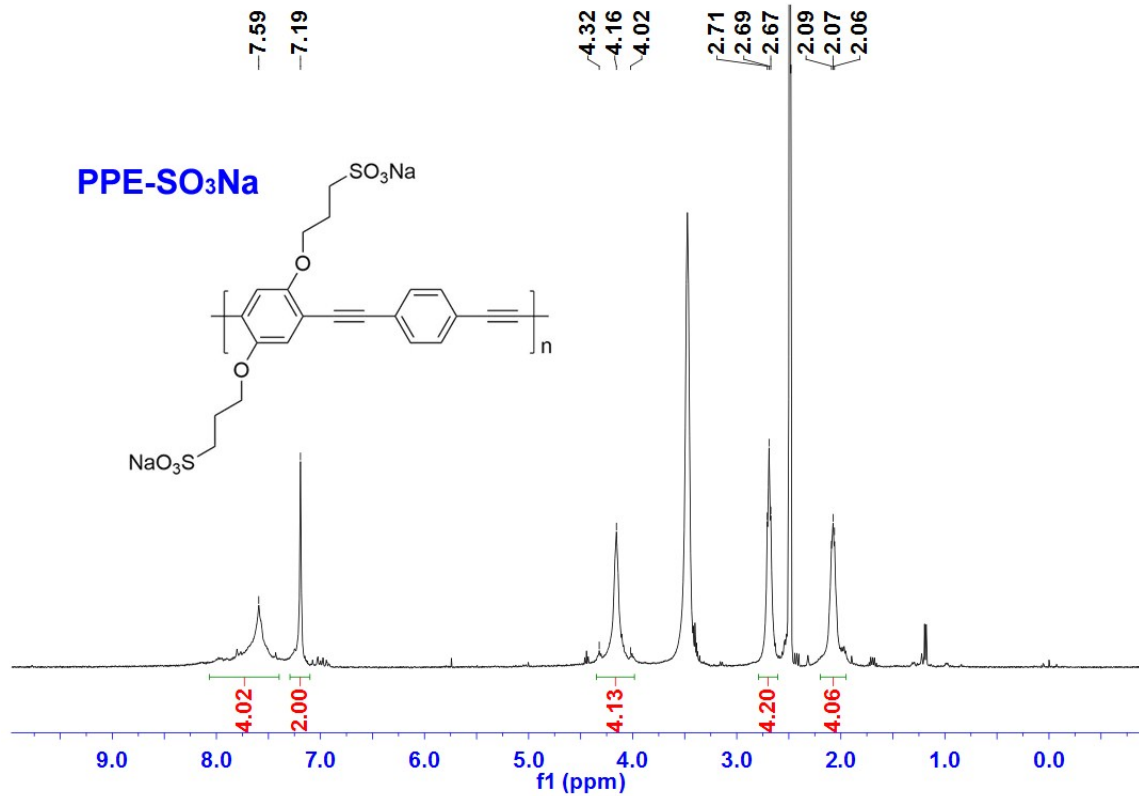


**Figure S23.** TEM images of NDI-Bola/PPE-SO<sub>3</sub>Na (10:1, n/n) at (a) pH 3.5 and (b) pH 9.8 (adjusted from pH 3.5 with 1 M NaOH). (c) The dependence of fluorescence emission of NDI-Bola/PPE-SO<sub>3</sub>Na (10:1, n/n) and PPE-SO<sub>3</sub>Na (100 μM) excited at 420 nm in water. The concentration of NDI-Bola and PPE-SO<sub>3</sub>Na in the NDI-Bola/PPE-SO<sub>3</sub>Na composite was 1 mM and 100 μM, respectively. (d) ζ-potential titration of preformed NDI-Bola nanotubes (2 mM) in water at 25 °C.









**Target**  
 Target type  
 Target serial number  
 Position H11

**Laser**  
 Laser beam attenuation 14.815  
 Laser beam focus -1  
 Laser repetition rate 60 Hz  
 Number of shots 50

**Spectrometer**  
 positive voltage polarity POS  
 PIE delay 1000 ns  
 Ion source voltage 1 20 kV  
 Ion source voltage 2 17.65 kV  
 Lens voltage 9.3 kV  
 Linear detector voltage 1.751 kV  
 Deflection on true  
 Deflection mass 5000 Da

MSMS parent mass  
 LIFT voltage 1  
 LIFT voltage 2  
 LIFT 1 Pulser time depending on the parent mass  
 LIFT 2 Pulser time

Reflector voltage 1 0 kV  
 Reflector voltage 2 0 kV  
 Reflector detector voltage 0 kV

**Instrument**  
 Instrument type microflex  
 Serial instrument number BA070061  
 Name of computer MASS-FLEX  
 Operator ID or name j1349  
 flexControl version flexControl 3.3.108.0  
 flexAnalysis version

Date of Acquisition 2017-04-06T18:43:30.922-04:00  
 Acquisition method D:\Methods\flexControl\Methods\LP\_40-150kDa.par  
 Processing method  
 File Name D:\DATA\Parquette\Mingyang\PPE-SO<sub>3</sub>Na\_20170406\SA\_LP40-150kDa\0\_H1112

Performed by	Viewed by
Date / Sign	Date / Sign

**BRUKER DALTONICS**  
 printed: 4/6/2017 6:50:10 PM

## References

1. Liu, J.; Rinzler, A. G.; Dai, H.; Hafner, J. H.; Bradley, R. K.; Boul, P. J.; Lu, A.; Iverson, T.; Shelimov, K.; Huffman, C. B., Fullerene pipes. *Science* **1998**, *280* (5367), 1253-1256.
2. Shao, H.; Seifert, J.; Romano, N. C.; Gao, M.; Helmus, J. J.; Jaroniec, C. P.; Modarelli, D. A.; Parquette, J. R., Amphiphilic Self - Assembly of an n - Type Nanotube. *Angew. Chem. Int. Ed.* **2010**, *49* (42), 7688-7691.
3. Tan, C.; Pinto, M. R.; Schanze, K. S., Photophysics, aggregation and amplified quenching of a water-soluble poly (phenylene ethynylene). *Chem. Commun.* **2002**, (5), 446-447.
4. Zhang, T.; Fan, H.; Zhou, J.; Liu, G.; Feng, G.; Jin, Q., Fluorescent conjugated polymer PPES03: a novel synthetic route and the application for sensing protease activities. *Macromolecules* **2006**, *39* (23), 7839-7843.
5. Young, T.; Monclus, M.; Burnett, T.; Broughton, W.; Ogin, S.; Smith, P., The use of the PeakForce™ quantitative nanomechanical mapping AFM-based method for high-resolution Young's modulus measurement of polymers. *Meas. Sci. Technol.* **2011**, *22* (12), 125703.
6. Criado, M.; Rebollar, E.; Nogales, A.; Ezquerro, T. A.; Boulmedais, F.; Mijangos, C.; Hernández, R., Quantitative Nanomechanical Properties of Multilayer Films Made of Polysaccharides through Spray Assisted Layer-by-Layer Assembly. *Biomacromolecules* **2016**, *18* (1), 169-177.
7. Fantini, C.; Jorio, A.; Souza, M.; Strano, M.; Dresselhaus, M.; Pimenta, M., Optical transition energies for carbon nanotubes from resonant Raman spectroscopy: Environment and temperature effects. *Phys. Rev. Lett.* **2004**, *93* (14), 147406.
8. Smolyakov, G.; Pruvost, S.; Cardoso, L.; Alonso, B.; Belamie, E.; Duchet-Rumeau, J., AFM PeakForce QNM mode: Evidencing nanometre-scale mechanical properties of chitin-silica hybrid nanocomposites. *Carbohydr. Polym.* **2016**, *151*, 373-380.